ARL 45

PRESSURE ENERGY EXCHANGE PRINCIPLE

JOHN E. MINARDI
CHARLES E. PAX
HAROLD E. WRIGHT

RESEARCH INSTITUTE
UNIVERSITY OF DAYTON
DAYTON, OHIO

MAY 1961

CONTRACT AF 33(616)-6417

AERONAUTICAL RESEARCH LABORATORY
OFFICE OF AEROSPACE RESEARCH
UNITED STATES AIR FORCE

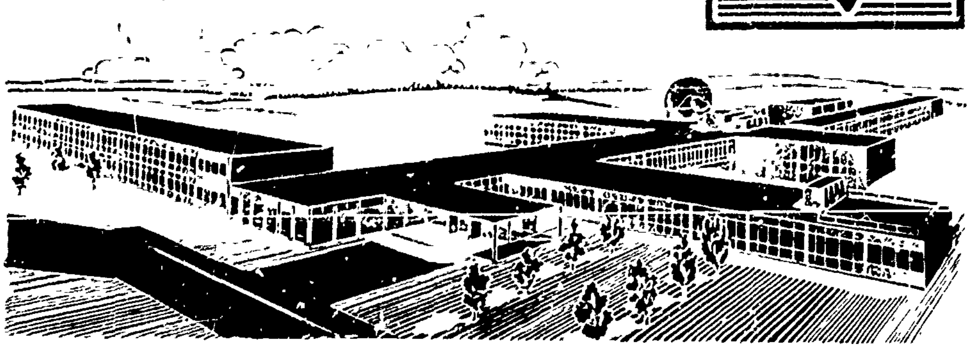

NOTICES

ARL 45

PRESSURE ENERGY EXCHANGE PRINCIPLE

John E. Minardi
Charles E. Pax
Harold E. Wright

Research Institute
University of Dayton

May 1961

Contract No. AF 33(616)-6417
Project No. 7063
Task No. 70151

Aeronautical Research Laboratory
Office of Aerospace Research
United States Air Force
Wright-Patterson Air Force Base, Ohio

FOREWORD

This interim technical documentary report was prepared by the University of Dayton Research Institute, Dayton, Ohio, on Air Force Contract AF 33(616)-6417. This contract was initiated under Project No. 7063, "Mechanics of Flight" and Task No. 70151, "Investigation of Internal Visco-Compressible Flow Phenomena." The work was administered under the direction of the Fluid Dynamics Research Branch of the Aeronautical Research Laboratory. Mr. Maurice O. Lawson was the ARL Project Engineer for this work.

The able assistance and cooperation of the members of the Aeronautical Research Laboratory and in particular the efforts of Mr. Lawson, Dr. Hans J. P. von Ohain and Dr. Roscoe H. Mills are appreciated and hereby acknowledged.

The work described in this technical note was conducted in the period 15 April 1960 to 14 April 1961.

ABSTRACT

Pressure energy exchange principles are being investigated by the University of Dayton Research Institute. These studies are directed toward achieving temperatures of the order of 10,000°R in substantial amounts of uncontaminated, high pressure air, and higher temperatures in small amounts of air.

A system using high pressure air to raise the temperature of a charge of air by rapid compression up to 200 atmospheres is being used for experimental studies. Also being investigated is a system which uses a column of water at velocities up to two hundred feet per second to compress a charge of air. A brief description of both systems and the preliminary results from the first few experimental tests are included in this Technical Note. A theoretical development of conditions resulting from shock heating of the charge gas is presented.

TABLE OF CONTENTS

LIST OF FIGURES

LIST OF SYMBOLS

a	Speed of sound
A	Area
B	A boundary layer heat transfer function
c_p	Specific heat at constant pressure
d	Distance along body
D	Diameter
g	32.2 ft/sec.^{2}
ℓ	Distance along body
m	Mass
M	Mach number
n	Polytropic exponent; number of shock waves which have traveled through the gas
P	Pressure
P_r	Prandtl number
q	Heat transfer rate per unit area
Q	Total heat transfer
S	Distance
t	Time (seconds)
T	Temperature
T_R	Recovery temperature
T_W	Wall temperature
u	Internal energy; velocity
V	Volume; velocity
W	Weight
X	Distance
γ	Specific heat ratio $= C_p/C_V$

LIST OF SYMBOLS (CONT'D)

θ	Swirl angle
μ	$\gamma + 1/\gamma - 1$
λ	$\mu + 1/P_{1S}/P_{1c} - 1$
Γ	Gamma function
ρ	Density
τ	Time

Subscripts

a	Annex
c	Charge
D	Driver
f	Final
L	Refers to laminar boundary layer
n	Refers to conditions after n shocks
t	Conditions in shock tube
T	Refers to turbulent boundary layer
ch	Refers to charge gas initially in compression chamber
p	Piston
S	After shock wave
1	Initial conditions; conditions after first shock
2	Conditions after second shock

Superscripts

*	Refers to throat conditions

SECTION I

INTRODUCTION

Laboratory methods of obtaining temperatures of the order of 10,000° Rankine in gases are of ever increasing importance. The presence of even small amounts of impurities in these gases is undesirable since some properties of high energy gases can be greatly affected by traces of other materials. The amount of high energy gas available and its pressure also determine to a very large degree both the instrumentation requirements and the types of problems which can be simulated in the laboratory.

A method which might produce the desired conditions in a large amount of air was demonstrated at the Aeronautical Research Laboratory by Mr. M. O. Lawson. This low pressure system was further tested by the University of Dayton and is described in detail in Reference 1. The results of these tests were utilized in designing a higher energy system operating at pressures up to 200 atmospheres.

This technical note describes the development, construction, and operation of this 200 atmosphere system as well as theoretical and initial test performance. Also described are systems which utilize the kinetic energy of a piston or column of water to compress a small amount of air to high energy density.

Manuscript released May 1961 by the authors for publication as an ARL Technical Documentary Report.

SECTION II

DESCRIPTION OF APPARATUS

GAS DRIVER SYSTEM

The physical arrangement of the 200 atmosphere pressure energy exchange system is shown in Figure 1. The basic concept of operation is the use of a large amount of "driver" gas at a low energy density to produce a high energy density in a smaller amount of "charge" gas. This is accomplished by allowing the higher pressure driver gas to compress the charge gas and thereby add energy to the charge gas.

It is clear that the final temperatures achieved in the charge gas will be influenced by the amount of mixing of the lower temperature driver gas with the high final temperature charge gas as well as heat losses and the compression process itself. In order to more clearly describe this system it can be divided into the following sections:

1. Compression Chambers and Preheater Assembly
2. Shock Tube Section
3. Diaphragm Assembly
4. Air Treatment and Storage System
5. Instrumentation and Control System

A brief description of each of these sections follows.

<u>Compression Chambers and Preheater Assembly</u>

The compression chambers consist of a 6" diameter x 6" long main chamber and a smaller annex chamber (Figure 2). Design values of the geometric parameters of V_a/V_t A^*/V_t and θ are those which optimized performance of the low pressure system previously investigated. These geometric parameters are variable in steps to permit investigation of their influence upon performance. Preheating of the charge air in the compression chambers is accomplished by Nichrome heating elements which form the inner surfaces of the chambers.

Immediately down stream the main chamber orifice is an air operated piston which serves as a quick opening valve to initiate flow into the compression chambers. This valve is opened by venting the cylinder behind the piston to atmosphere. Since the piston area exposed to the driver gas before the valve begins to open is only 25% of the total piston area, the cylinder pressure is much lower than driver pressure. When the valve begins to open the entire area is exposed to driver pressure so that the valve opens quickly and remains completely open. Opening time is estimated to be several milliseconds. This time is a small fraction of the total compression time and since the compression chamber and entrance configurations do not favor shock heating of the gas in the chamber there would be little advantage in using conventional diaphragm rupture to release the driver gas instead of the above valve. The need of replacing diaphragms after each operation is thereby eliminated with this configuration.

The entering driver air is directed to the periphery of the chamber and upon passing through the swirl vanes enters the main chamber. The tangential motion

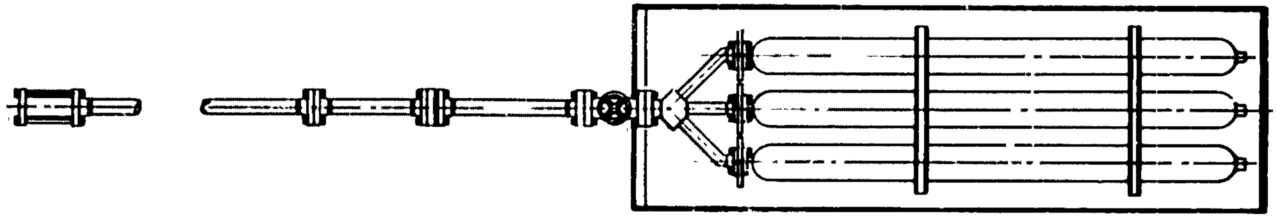

Figure 1. 200 Atmosphere System Layout

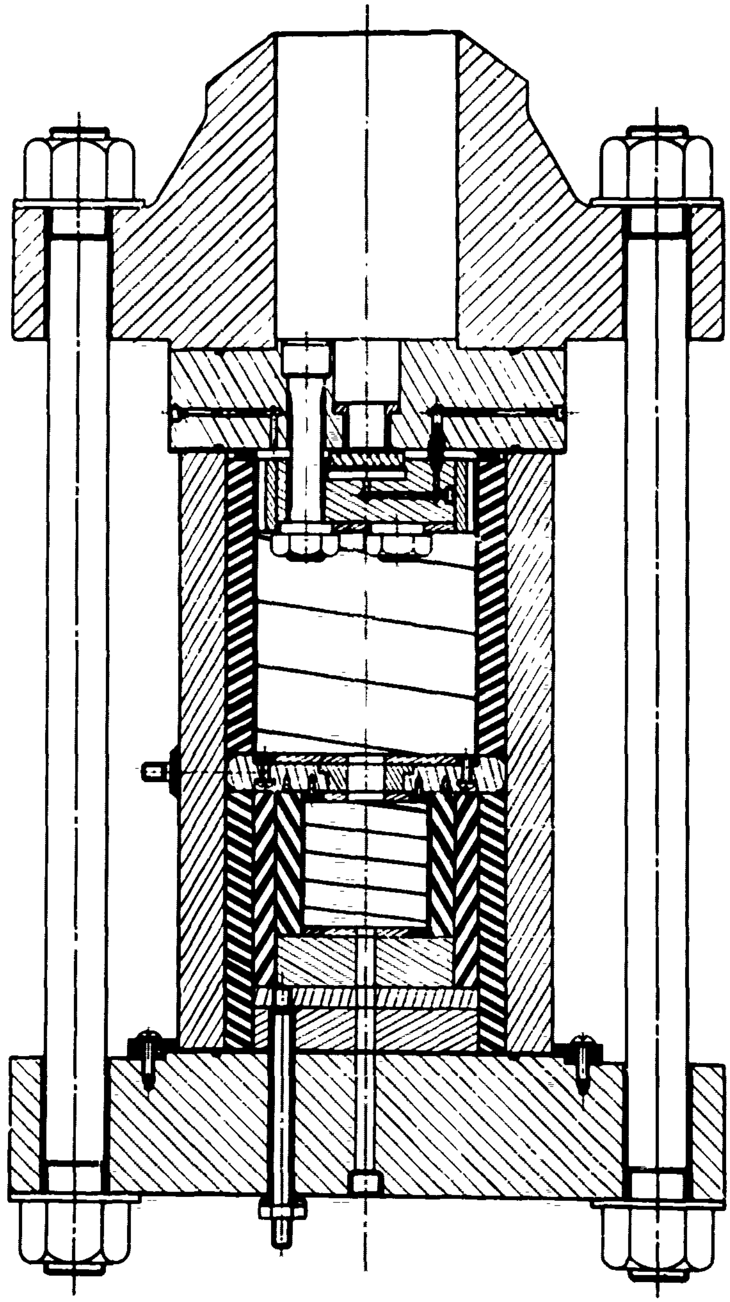

Figure 2. Gas Compression Chamber

of the driver air tends to keep it to the outside of the main chamber and thus reduces the amount of driver air which enters the annex chamber and mixes with the charge gas.

Shock Tube Section

The shock tube section is a 27 foot length of commerical high pressure pipe with internal diameter of 4.9 inches. This tube is part of the storage system when the quick-opening valve is used as described previously. For studies involving shock heating of the charge gas, this tube becomes part of the initial charge volume, the quick-opening valve remains open, and diaphragm rupture is used to initiate flow. This tube then initially contains the major portion of the charge gas which upon rupture of the diaphragm is heated and compressed first by primar, and reflected shock waves in the tube and then by final compression in the compression chambers.

Mixing of charge and driver air during this final compression is reduced by keeping the final position of the ideal unbroadened interface well outside the chambers. The actual diffusion broadened interface is therefore largely outside the chamber and mixing after final compression must be by diffusion through the small area of the inlet orifice. Any portion of the diffused interface which enters the chamber during the compression process is retarded from mixing with the charge gas in the annex chamber by the swirl imparted to this gas upon entering the main chamber.

Diaphragm Assembly

The diaphragm assembly gives controlled rupture throughout the testing range of pressures. This assembly, shown in Figure 3, clamps two diaphragms separated by a spacer. Required diaphragm clamping force is developed by a floating annular piston which clamps both diaphragms when the tube upstream of the diaphragms is pressurized (Reference 2). Initial clamping to insure sealing is furnished by bolting of flanges. The diaphragm section is pressurized so that each diaphragm carries about one-half the total driver pressure. The six inch gate valve to the stored driver air can then be opened without surge loading of the diaphragms. To initiate rupture of the diaphragms the full driver pressure is bled into the space between the diaphragms causing rupture of the downstream and upstream diaphragms in rapid succession.

Air Treatment and Storage System

The compressed driver air is filtered, and passed through units to remove oil and water vapor. The driver storage vessels which operate the system with less than a 10% pressure drop have a combined volume of 52.5 ft^3. This equipment is described in Reference 1.

Instrumentation and Control System

All controls are at a central location beyond concrete safety walls. The instrumentation and control panel is shown in Figure 4.

Air temperatures are presently being measured with .001 inch diameter chromel-alumel thermocouples, however, at higher temperatures 60 percent

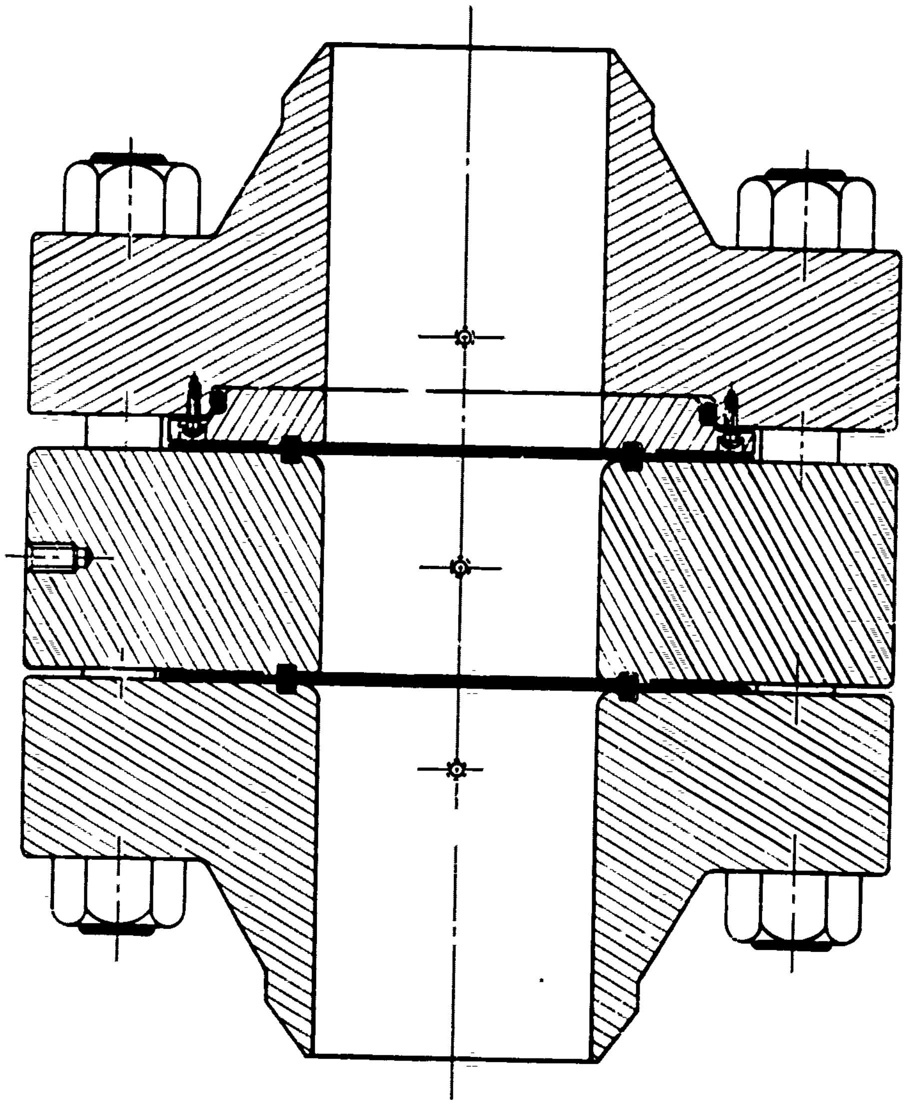

Figure 3 Diaphragm Assembly

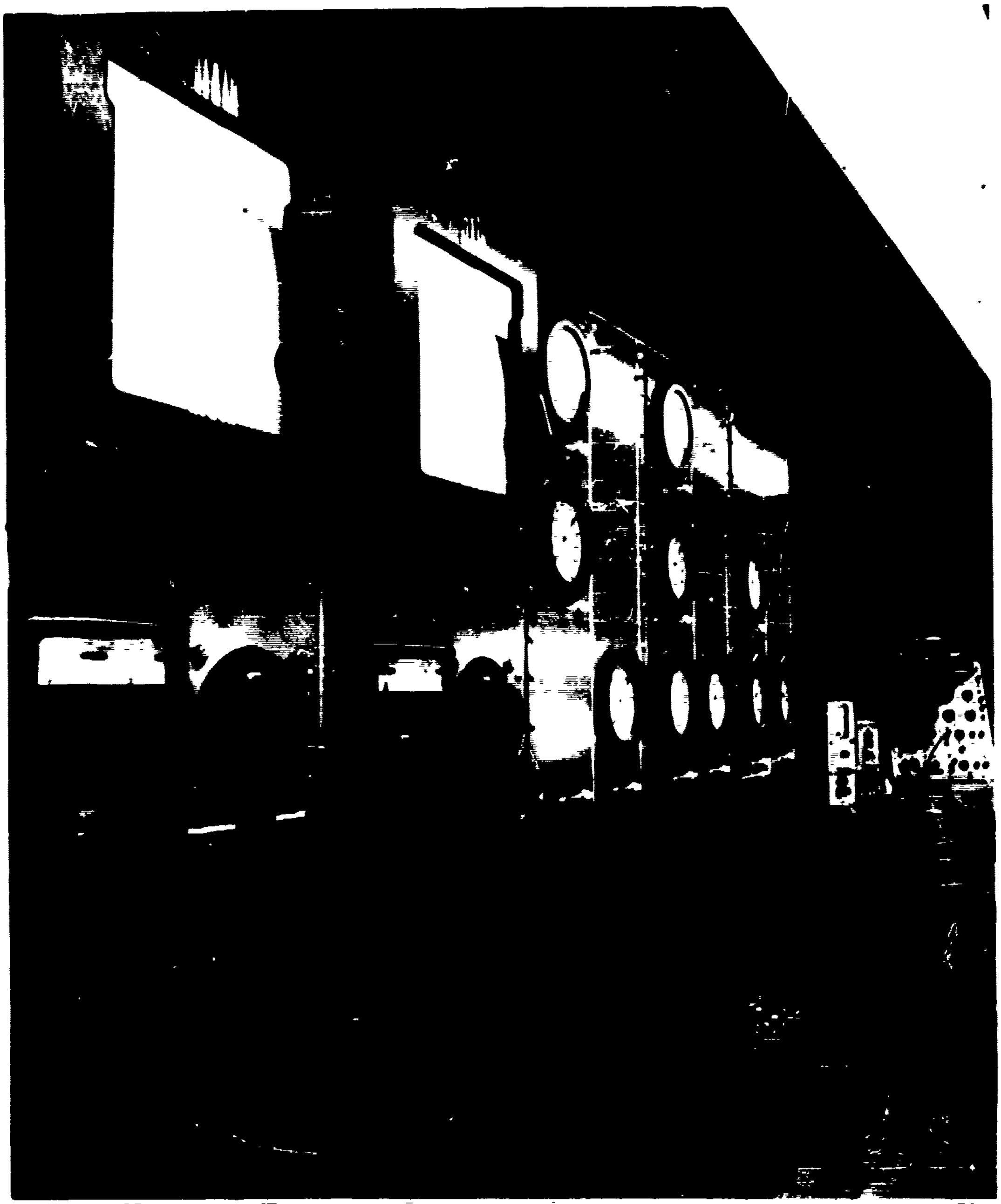

Figure 4. Instrumentation and Control Panel

Irridium 40 percent Rhodium thermocouples will be used. Temperatures during preheating and cooling after compression are recorded on strip chart recorders while the more dynamic temperatures encountered during the compression process are recorded on an oscilloscope. A dynamic pressure transducer gives pressure history of the charge gas in the compression chamber. Static pressures of all portions of the system are displayed at the panel and controlled with solenoid or motor operated valves. The 200 atmosphere system was completed and shakedown operations began in December of 1960.

LIQUID DRIVER SYSTEM

A low pressure liquid driver system, Figure 5, utilizing water as the driver medium and air as the charge gas was designed for driver fluid pressure of 300 psi while the initial charge gas pressure can be varied from below atmospheric to driver liquid pressure. The construction of the system has been completed and shakedown tests are now being performed.

The system is composed of three essential elements: driver liquid storage tank, ram tube, and compression chamber. These are described in the following paragraphs.

Driver Liquid Storage Tank

The driver liquid storage tank is a 500 psi pressure vessel with a volume of eight cubic feet. Pressure on the driver fluid is maintained by an air cushion. The ratio of air cushion volume to initial charge gas volume is maintained so that the pressure on the driver liquid does not drop more than five percent during a test.

Ram Tube

The ram tube connects the driver liquid storage tank to the compression chamber. The function of this tube is to permit the high pressure air cushion in the driver tank to accelerate a considerable amount of driver liquid which then compresses the charge gas to a pressure which is much higher than the pressure of the air cushion in the driver tank. As the charge gas forces some of the driver liquid back into the storage tank the pressure oscillates back to driver pressure. In addition to the diaphragm at the storage tank used to initiate flow the ram tube is equipped to receive a diaphragm near the compression chamber. This permits initial evaculation of the ram tube in order to increase liquid driver velocity.

The tube has an internal diameter of one inch and a length which can be varied from one foot to 20 feet. With the exception of short sections near the diaphragms the tube is transparent plastic to permit visual and photographic observation.

Compression Chamber

The compression chamber (Figure 6) is a 6 inch internal diameter cylinder into which driver liquid enters tangentially at the periphery. The ends of the cylinder are transparent to permit visual and photographic observation of the compression process.

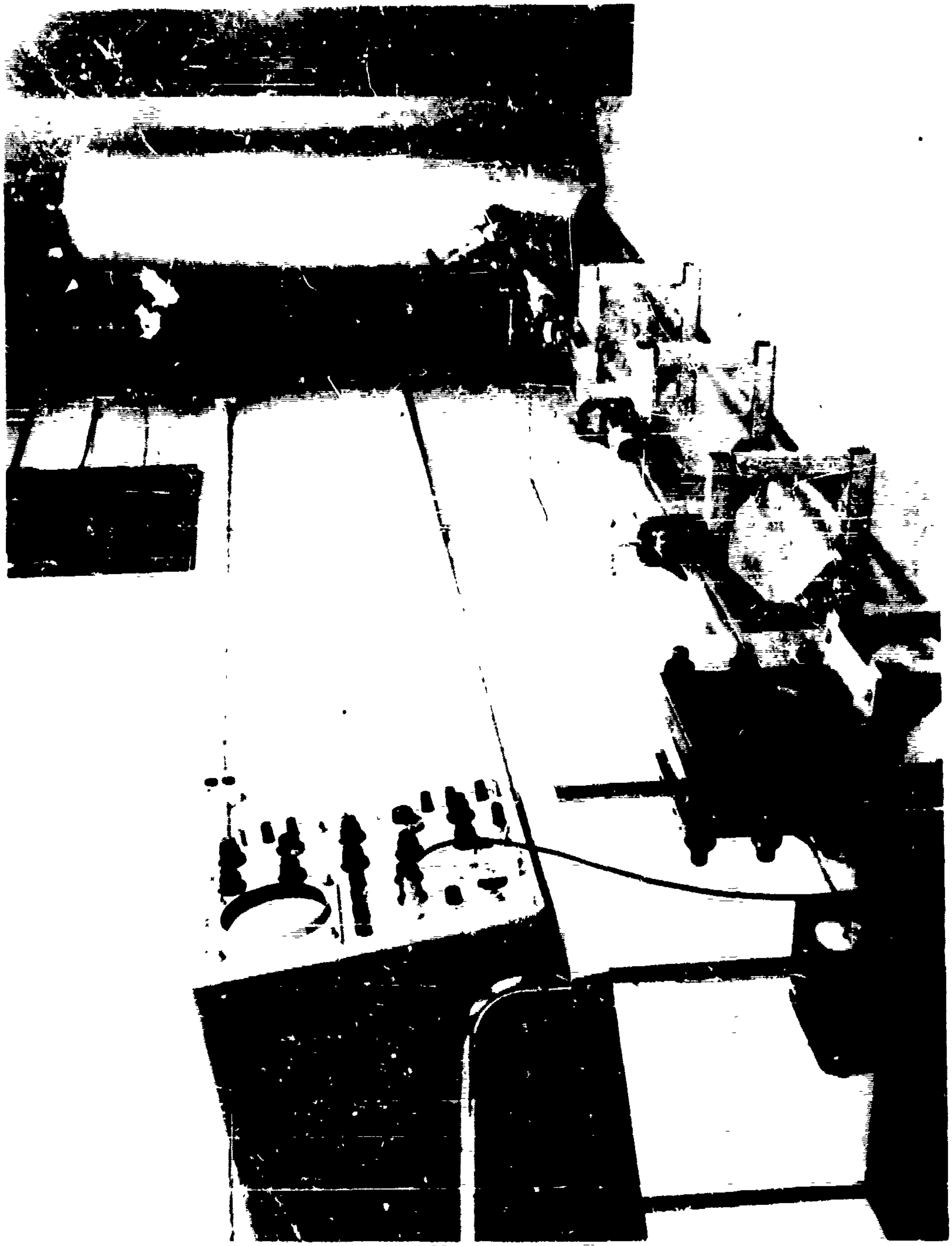

Figure 5. Liquid Driver System

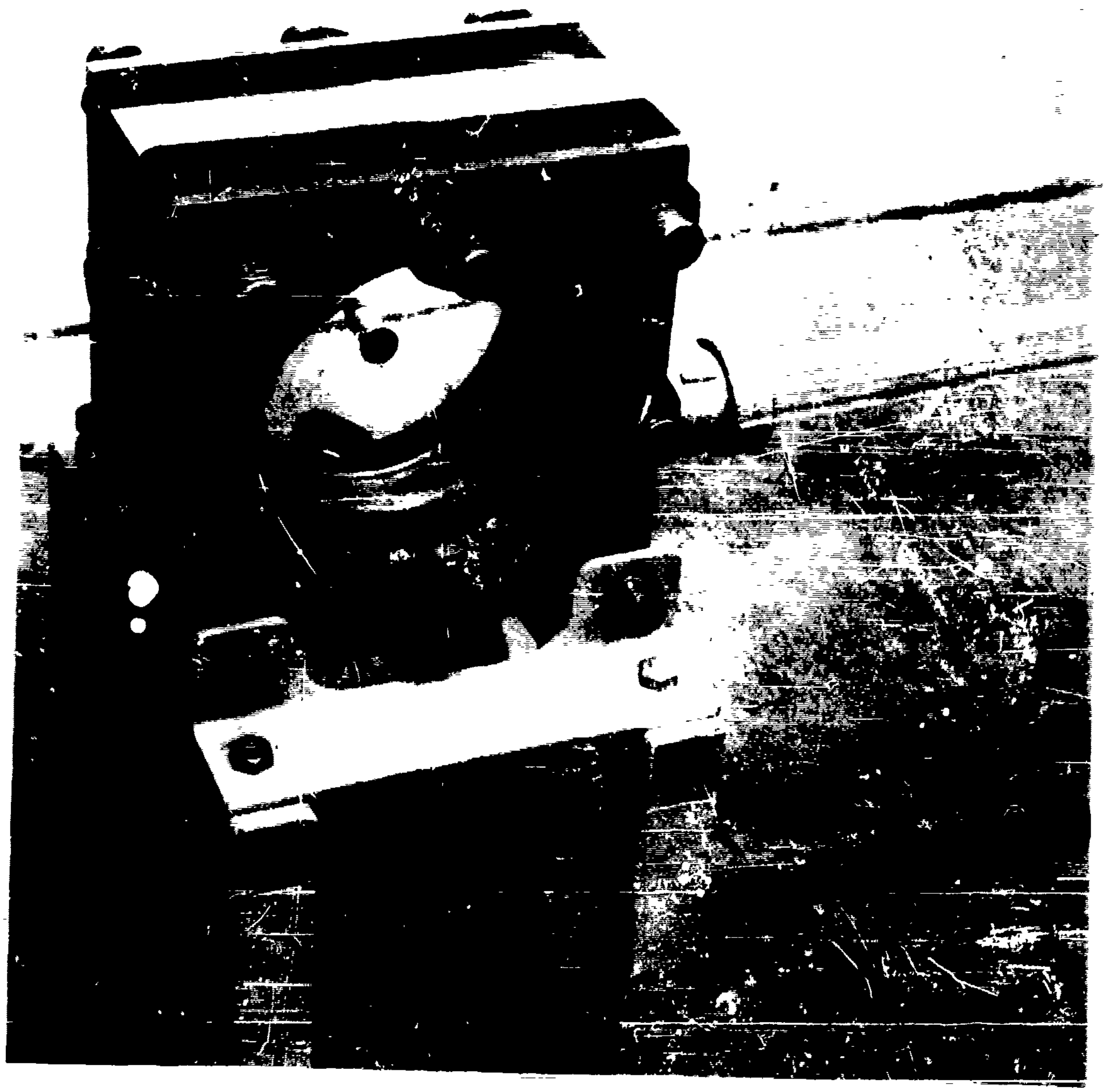

Figure 6. Liquid Driver Compression Chamber

SECTION III

RESULTS AND DISCUSSION

The systems being investigated for producing high energy air can be separated into three categories depending on the driving system. These are liquid driven, gas driven, and solid piston driven systems. Each of these types of systems is treated here.

Gas Driven Systems

One of the gas driven systems being tested ideally brings the charge gas to driver pressure by means of isentropic compression, whereas the second system ideally brings the charge gas to driver pressure through two shocks and a final stage of isentropic compression. The 200 atmosphere non-shock system is very similar in operating principles to the low pressure system described in Reference 1. Therefore, the theoretical performance of this system will not be repeated in this report. Some test data obtained with the 200 atmosphere system are compared with theoretical performance and previous data from the low pressure system in Figure 7.

One mil chromel-alumel thermocouples have been used to date to measure charge air temperatures. Three thermocouples in parallel are used to average out local temperature differences. In case of breakage of one of these thermocouples the data for that test is still usable. Breakage of thermocouples has not been a problem with the nonshock configuration, but has been quite bothersome with the shock configuration. Most of the breakage has been caused by flexing of the support rods used on the thermocouple probe and impact of scale particles on the thermocouple wires. A more rugged probe and general cleaning of the system should correct these conditions. Operation of the quick opening valve is now satisfactory after some initial difficulties with leakage past the valve. Preheating of the charge gas has not been satisfactory and a larger power supply is required to obtain the desired temperatures.

On the second system described above the shocks will increase the entropy of the charge gas while the final pressure will still be driver pressure, hence the temperature will be higher. The theoretical development of such a system is described here.

When the diaphragm is ruptured and a shock travels down the tube and strikes the inlet plate to the compression chamber, the shock is reflected back up the tube toward the interface shock heating the larger portion of the charge a second time. Even though further shocks may occur in the tube the major portion of the entropy increase will have already occurred, hence the remainder of the process will be nearly isentropic assuming no heat losses. Influence of heat losses in the compression chamber can be accounted for by proper choice of the polytropic exponent for the final portion of compression. The reflected shock will essentially have the strength associated with reflection from a closed end tube since the ratio $A_t/A^* = 24$ (see Reference 3).

With the following assumptions:

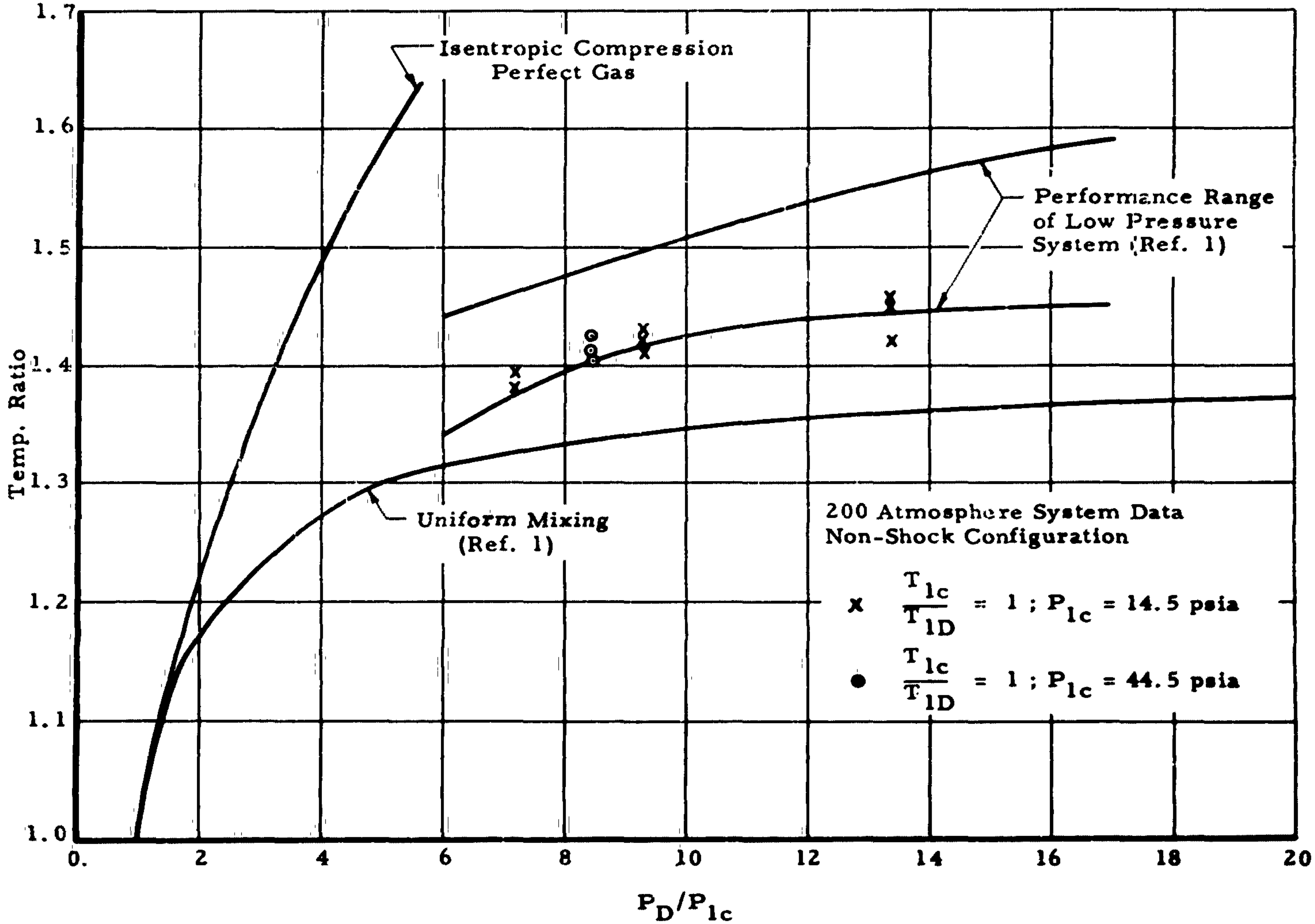

Figure 7. Performance of Non-Shock System

(a) Perfect gases
(b) No shock attenuation
(c) No heat losses

the following equations can be used to determine the final gas properties. From Reference 4 the relation between shock Mach Number and pressure ratio across the diaphragm is

$$\frac{P_D}{P_{1c}} = \frac{1}{\mu_c}\left[\frac{2\gamma_c}{(\gamma_c - 1)} M_S^2 - 1\right]\left[1 - \frac{\gamma_D - 1}{\gamma_c + 1}\left(\frac{a_c}{a_D}\right)\frac{M_S^2 - 1}{M_S}\right]^{-\frac{2\gamma_D}{\gamma_D - 1}} \tag{1}$$

The pressure ratio across the first shock is:

$$\frac{P_{1S}}{P_{1c}} = \frac{2\gamma}{\gamma + 1} M_S^2 - \frac{1}{\mu} . \tag{2}$$

Using the equations from Evans and Evans (Reference 5) the remaining properties behind both shocks can be obtained. These equations were obtained for a constant velocity piston traveling down a closed end tube. The shock wave generated by the piston motion would reflect from the closed end, then from the piston etc. Then:

$$\frac{P_{nS}}{P_{1c}} = \frac{\Gamma(\lambda)\,\Gamma(\lambda + \mu + n + 1)}{\Gamma(\lambda + \mu + 1)\,\Gamma(\lambda + n)} \tag{3}$$

$$\frac{\rho_{nS}}{\rho_{1c}} = \frac{\Gamma(\lambda + 1)\,\Gamma(\lambda + \mu + n)}{\Gamma(\lambda + \mu)\,\Gamma(\lambda + n + 1)} \tag{4}$$

$$\frac{T_{nS}}{T_{1c}} = \frac{(\lambda + n)(\lambda + \mu + n)}{\lambda(\lambda + \mu)} \tag{5}$$

$$u_{nS} = u\left(\frac{\lambda + n}{\mu - 1} + c\right) \quad c = \begin{cases} 0 \text{ if } n \text{ even} \\ 1 \text{ if } n \text{ odd} \end{cases} . \tag{6}$$

The subscript, n, refers to conditions behind the nth shock. U_{nS} is nth shock velocity relative to the fixed tube and Γ is the gamma function. With assumptions a, b, and c these equations also hold for the first shock and reflected shock in the shock tube since the interface progresses down the tube at constant velocity until it collides with the reflected shock.

If n = 2 is substituted into equation (4) we have

$$\frac{P_{2S}}{P_{1c}} = \frac{P_{1S}}{P_{1c}}\left(\frac{\lambda + \mu + 2}{\lambda + 1}\right). \tag{7}$$

The final temperature ratio is obtained by the familiar isentropic compression formula

$$\frac{T_{f_c}}{T_{1c}} = \frac{T_{2S}}{T_{1c}}\left(\frac{P_D}{P_{2S}}\right)^{\frac{\gamma - 1}{\gamma}} \tag{8}$$

Points for Figure 8 were calculated using this model where T_f/T_{1c}, T_{2S}/T_{1c}, and T_{1S}/T_{1c} are plotted versus shock Mach Number. Also shown are real gas effects. Data for these curves were obtained from References 6, 7, and 8. With no modifications the present configuration can obtain a shock Mach Number of 2.6 traveling into atmospheric air, however, if the charge gas initial pressure is reduced to 10^{-2} atmospheres a shock Mach Number of 4.0 could be achieved.

The gas which is in the compression chamber can be preheated and the question arises whether or not it is desirable to mix this gas with the shock heated gas entering the compression chamber.

Initially, with preheating, the gas in the tube and in the compression chamber are at the same pressure but different temperatures. Further it is assumed that the gas in the compression chamber is isentropically compressed while the gas in the shock tube is compressed as described above. Using conservation of mass and energy the following equation for the "cup mixing" temperature is obtained

$$T_{f_c} = \frac{\frac{P_D}{P_{1c}} T_{1ch} T_{ft}}{\frac{P_D}{P_{1c}} T_{1ch} + T_{ft} - T_{fch}}.$$

From the assumed isentropic compression in the compression chamber:

$$T_{f_c} = \frac{\frac{P_D}{P_{1c}} T_{1ch} T_{ft}}{\frac{P_D}{P_c} T_{1ch} + T_{ft} - \left(\frac{P_D}{P_{1c}}\right)^{\frac{\gamma - 1}{\gamma}} T_{1ch}} \tag{9}$$

now:

$$T_f > T_{ft} \text{ if } T_{ft} - \left(\frac{P_D}{P_{1c}}\right)^{\frac{\gamma - 1}{\gamma}} T_{1ch} < 0$$

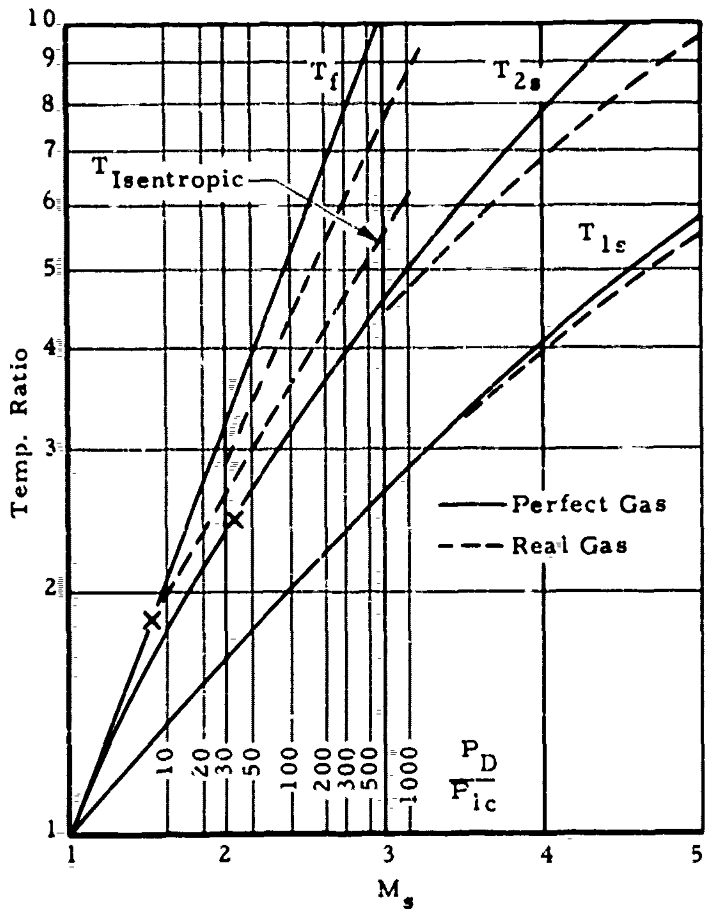

Figure 8. Theoretical Temperature Ratios for Air without Heat Losses

and

$$T_f < T_{ft} \quad \text{if} \quad T_{ft} - \left(\frac{P_D}{P_{1c}}\right)^{\frac{\gamma - 1}{\gamma}} T_{1ch} > 0 .$$

Then

$$\frac{T_{1ch}}{T_{1t}} = \frac{T_{ft}}{T_{1t}} \frac{1}{\left(\frac{P_D}{P_{1c}}\right)^{\frac{\gamma - 1}{\gamma}}} ; \tag{10}$$

which enables one to judge the desirability of mixing in the compression chamber when preheating. Figure 9 is a plot of equation (10). For values of preheat above the curve no mixing is desirable; for values below the curve, mixing in the compression chamber is desirable. Hence the compression chamber of the non-shock configuration is desirable for values of T_{1ch}/T_{1t} above the curve of Figure 9 while a simpler collecting chamber would be desirable for values of T_{1ch}/T_{1t} below the curve since some heat sinks could be eliminated. It should be noted that the position of the curve was calculated using the model for T_{ft}/T_{1t} as given above.

Estimated heat losses from the shock heated gas can be calculated by the method of Reference 9. This analysis uses the heat transfer for steady flow past a flat plate at the velocity u behind the shock. The conditions of the boundary layer with time after shock passage at any point in the shock tube can be related to a position on the flat plate. In Figure 10 the conditions of the boundary layer at time t and point p are the same as the conditions at the distance d on the flat plate therefore

$$u_S t + d = u_S \frac{d}{u} \qquad\qquad d = \frac{u_S}{u_S - u} \; ut .$$

This is the relation between d and t required to use the steady flow equation for a flat plate.

For the laminar flow case according to Reference 9 the heat loss rate is

$$q_L = B_L t^{-0.5}$$

where

$$B_L = (T_R - T_W) \left[\frac{1}{\pi} (K\rho\, c_p)_{Wg} \left(1 - (\sqrt{2} - 1) \frac{u}{u_S}\right)\right]^{0.5}$$

and

$$t = \tau - \frac{x}{u_S}$$

where t is the time after the shock passes the station x, and τ is the time after shock initiation. So

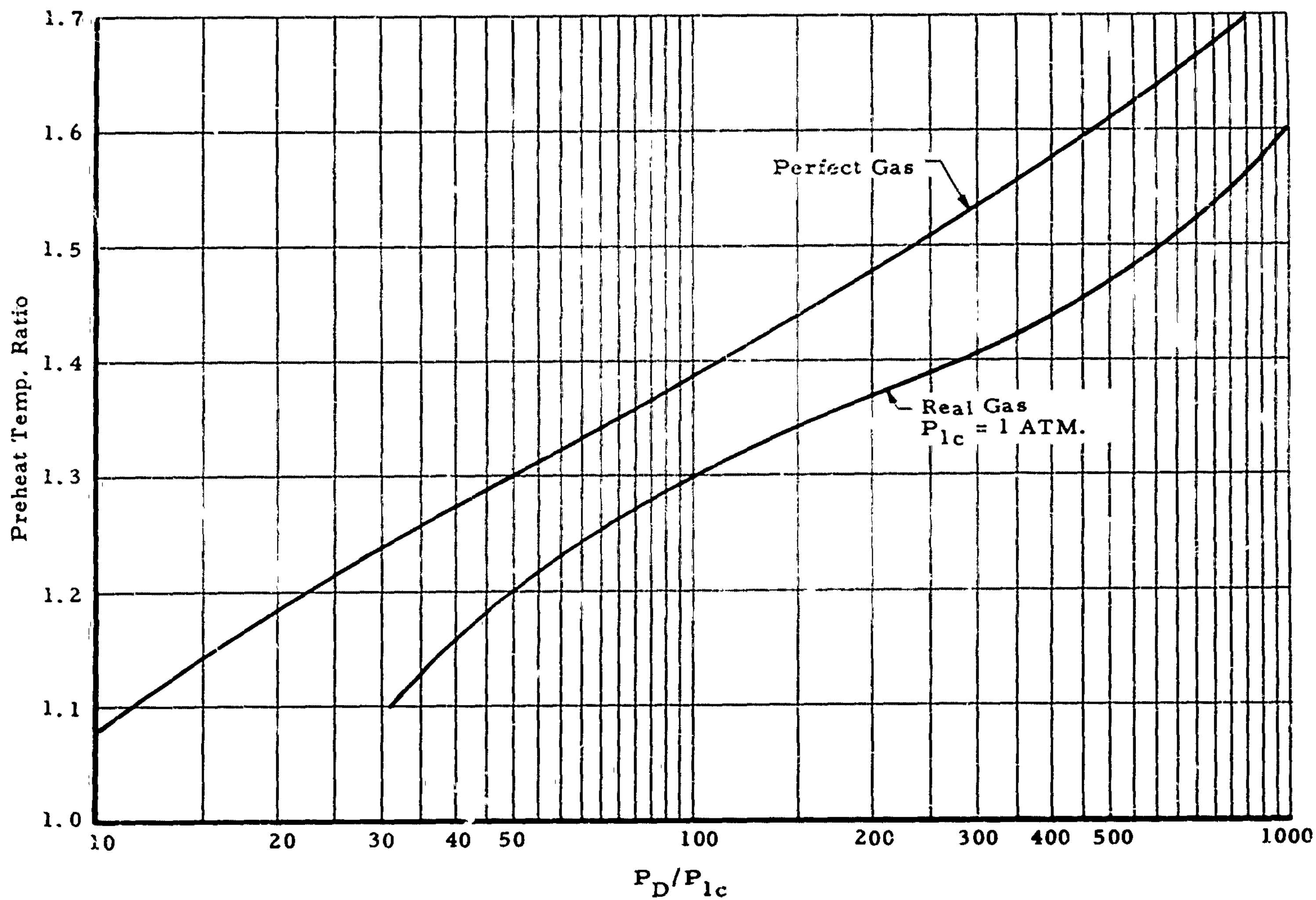

Figure 9. Mixing Criteria with Preheat

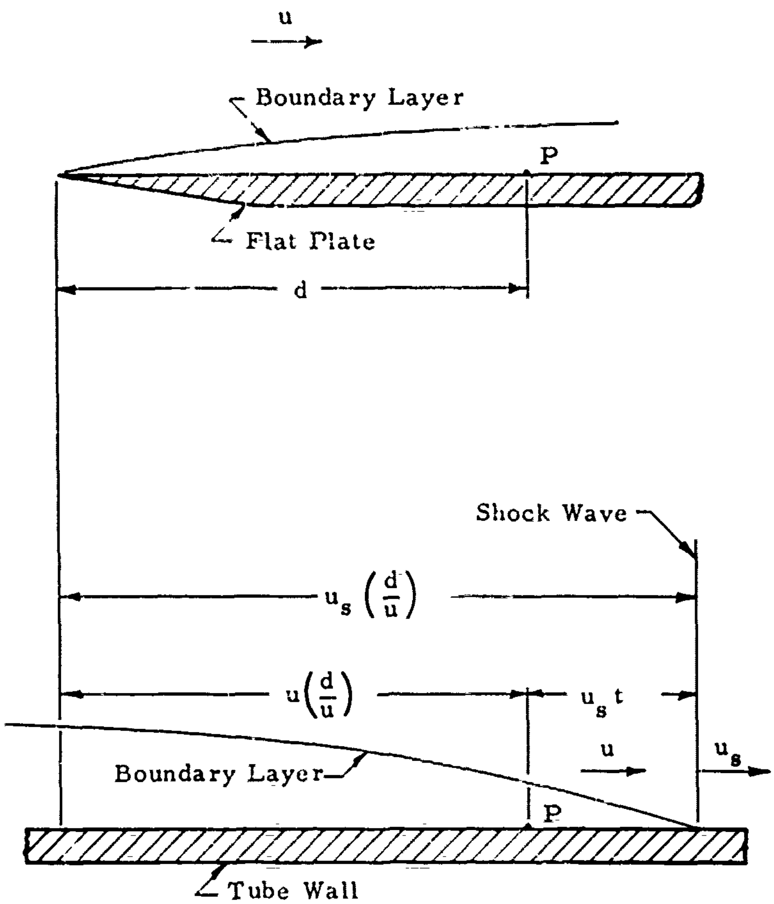

Figure 10. Flat Plate Analogy

$$Q_L = \int_0^S \int_{\frac{x}{u_S}}^{\frac{x}{u}} \pi D B_L \left(\tau - \frac{x}{u_S}\right)^{-0.5} d\tau dx + \int_S^{\ell} \int_{\frac{x}{u_S}}^{\frac{\ell}{u_S} + \frac{\ell - x}{u_{SR}}} \pi D B_L \left(\tau - \frac{x}{u_S}\right)^{-0.5} d\tau dx \qquad (11)$$

where the first term on the right represents the losses from those stations at which the loss starts at the time the shock passes (x/u_S) and ends at the time the interface passes (x/u). The second term represents the losses from those stations where losses by this mechanism end when the reflected shock passes ($\ell/u_S + \ell - x/u_{SR}$). The collision of the interface and the reflected shock occurs at station S.

After integration

$$Q_L = \frac{4}{3} \frac{\pi D B_L}{\sqrt{u_S}} S^{\frac{3}{2}} \left[\sqrt{\frac{u_S}{u} - 1} + \sqrt{1 + \frac{u_S}{u_{SR}}} \left(\frac{\ell}{S} - 1\right)^{\frac{3}{2}}\right] \qquad (12)$$

where

$$S = \ell\left(1 - \frac{\rho_{1c}}{\rho_{2S}}\right)$$

and

$$\frac{\ell}{S} - 1 = \frac{1}{\frac{\rho_{2S}}{\rho_{1c}} - 1}$$

Similarly for turbulent flow (Reference 9)

$$q_T = B_T t^{-0.2}$$

where

$$B_T = 0.0296 \left(T_R - T_W\right)\left(\frac{\bar{\mu}_{1S}}{\mu_{1S}}\right)^{0.2} \left(\frac{T_{1S}}{\bar{T}_{1S}}\right)^{0.8} \left(\frac{\bar{c}_{p1S}}{c_{p2S}}\right) \frac{\rho_{1S} c_{p1S} u}{P_r^{2/3}} \left(\frac{\mu_{1S}}{\rho_{1S} u u_S}\right)^{0.2} .$$

Therefore

$$Q_T = \frac{25}{36}\,\frac{\pi D B_T S^{1.8}}{u_S^{0.8}}\left[\left(\frac{u_S}{u} - 1\right)^{0.8} + \left(1 + \frac{u_S}{u_{SR}}\right)^{0.8}\left(\frac{\ell}{S} - 1\right)^{1.8}\right]. \qquad (13)$$

The cup mixing temperature for the air heated by the first shock is

$$\frac{T_{2\ell}}{T_{1c}} = \frac{T_{2S}}{T_{1c}} - \frac{\gamma - 1}{\gamma}\,\frac{Q}{P_{1c}V_{1c}} .$$

The loss behind the reflected shock is neglected since the time of this reflection is short and the velocity is essentially zero. The remainder of the compression is assumed to follow a polytropic process where $n = 1.3$ to account for heat losses. The final "cup mixing" temperature then is:

$$\frac{T_{f_c}}{T_{1c}} = \frac{T_{1\ell}}{T_{1c}}\,\frac{T_{2\ell}}{T_{1\ell}}\left(\frac{P_D}{P_{2S}}\right)^{\frac{n-1}{n}} . \qquad (14)$$

Solid Piston and Liquid Systems

A preliminary theoretical study was made of the use of a solid piston system for obtaining small amounts of uncontaminated gas at high temperature and pressure. One possible system uses a light gas gun (or ordinary gun) to fire a piston into an evacuated barrel. After the piston attains a high velocity it passes an array of vent holes which allows the driving gas to escape. The piston then pierces a diaphragm and compresses the charge gas. If it is desired that the charge gas remain confined an arrangement would be required to prevent reversal of the piston.

Any leakage encountered during compression would be from the charge gas since the driver pressure was vented, therefore, driver gas contamination is eliminated and piston clearance can be adequate to prevent serious heating problems due to friction with the walls when the piston is at high velocities. Since the compression process begins only after the piston has obtained maximum velocity the compression process would be very rapid and heat losses would be kept to a minimum.

If heat losses are neglected the total kinetic energy of the piston must be absorbed by the gas which is compressed in the barrel hence $m_c \, \Delta u = m_p V_p^2/2g$ then for a perfect gas

$$\frac{T_{f_c}}{T_{1c}} = 1 + \frac{W_p}{W_c}\,\frac{\gamma(\gamma - 1)}{2}\,M_p^2 . \qquad (15)$$

The final temperature, therefore, is a function of the weight ratio of piston to gas and the initial Mach Number of the piston relative to the charge gas. Since light-gas guns have fired light weight projectiles at velocities of 22,000 ft/sec, with proper weight ratio, small quantities of a perfect gas could be raised to temperatures of the order of 100,000 $^{\circ}$F. Of course, with real gas effects the temperature would be lower than indicated by equation (15).

It should be noted that equation (15) holds regardless of the irreversible processes which take place in the compression. A heavy, slow moving piston would more nearly approximate isentropic compression than a faster moving, lighter piston with the same kinetic energy, however, both would produce the same final temperature in the gas. The technique developed in Reference 5 can again be used to estimate final charge pressures.

This same solid piston model is applicable to the liquid system while the liquid is traveling as a solid in the ram tube. However, the liquid interface in the tube is unstable unless the liquid is accelerating. This can be accomplished by using a converging ram tube before the compression chamber.

The 300 psi liquid driver system has been operated with driver pressures up to 150 psi with initial charge gas pressure of one atmosphere. Peak charge pressures up to 600 psi were obtained, however, temperatures were not measured during these preliminary tests. Visual observation detected considerable entrainment at the liquid interface in the ram tube. Motion pictures will be used to study the nature and extent of this entrainment. Stable confinement of the compressed charge gas in the center of the compression chamber was maintained from one to three seconds.

SECTION IV

CONCLUSIONS AND RECOMMENDATIONS

Test data available at this time are of a preliminary nature. On the basis of these data and their agreement with predictions the following conclusions can be drawn.

1. Performance of the 200 atmosphere system operating in the non-shock configuration without preheating is in agreement with that predicted by the previous low pressure energy exchange system. When used in the shock configuration the performance is substantially improved.

2. In the liquid driver system, instability and entrainment are quite noticeable at the liquid interface in the ram tube.

It is recommended that testing of both air driven systems and the liquid system be continued.

Specifically for the gas driven systems the following recommendations are made:

1. The non-shock configuration should be tested using statistically designed experiments to determine:

   (a) The effects of preheat on performance.

   (b) The effects of higher absolute pressures on heat losses.

2. Tests with the shock configuration should be performed to determine:

   (a) The accuracy of the theoretical model in predicting performance.

   (b) The exact increases in performance over the non-shock configuration for a given pressure ratio.

   (c) The effect of preheat of charge gas in the compression chamber.

   (d) The effects of compression chamber configuration on performance.

3. Theoretical studies of the shock configuration should be made to determine the increased performance available utilizing gases such as helium as the driver gas.

4. Tests should be conducted with the shock tube and compression chamber partially evacuated.

Specifically for the liquid driven system the following recommendations are made.

1. High speed motion pictures should be taken of the interface in the ram tube and compression chamber with various operating conditions.

2. Tests should be performed to determine complete performance of the present configuration.

3. On the basis of data obtained from 1 and 2 above modifications of the ram tube and the compression chamber should be made to determine their effects on performance.

It is further recommended that theoretical studies and, if warranted, simple feasibility tests be performed on other systems which show promise of achieving the objectives of producing high temperature pure air.

REFERENCES

1. Minardi, J. E., C. E. Pax, and H. E. Wright. Research on Pressure Energy Exchange Principle. ARL TN 60-120, April 1960.

2. Cox, S. G. Development of the R. A. E. 6-inch Diameter Shock Tube, Part 1. Bursting of Diaphragms at 200 Atmospheres. R. A. E. TN Aero 2510, May 1957, Royal Aircraft Establishment, Farnborough, ASTIA Report No. AD 141 191.

3. Monroe, L. L. Investigation of the Transmission of a Shock Wave Through an Orifice. Guggenheim Aero. Lab. Memorandum No. 46, September 1958. ASTIA Document No. 139 322.

4. Glass, I. I. and J. G. Hall. Shock Tubes. University of Toronto, May 1958, UTIA Review No. 12. ASTIA Document No. 205 832.

5. Evans, C. and F. Evans. "Shock Compression of a Perfect Gas." Journal of Fluid Mechanics, October 1956, p. 399.

6. Gilmore, F. R. Equilibrium Composition and Thermodynamic Properties of Air to 24,000 °K. August 1955. ASTIA Document No. 84 052.

7. Shear, R. E. and P. McCane. Normally Reflected Shock Front Parameters. BRL Memo Report No. 1273, May 1960.

8. Logan, J. G., Jr. Thermodynamic Charts for High Temperature Air Calculations (2,000 °K to 9,000 °K). Cornell Aero Lab., July 1956. ASTIA Document No. 95 218.

9. Marrone, P. V., A. L. Russo, W. E. Smith, and R. C. Weatherston. Gasdynamics of a Wave Superheater Facility for Hypersonic Research and Development. February 1959. ASTIA Document No. 210 223.